Joint Beamforming and Power Splitting Design for Physical Layer Security in Cognitive SWIPT Decode-and-Forward Relay Networks

Xiaorong Xu*, Andi Hu, Yingbiao Yao, Wei Feng
School of Communication Engineering, Hangzhou Dianzi University
Hangzhou, Zhejiang 310018 - China
[e-mail: xuxr@hdu.edu.cn]
*Corresponding author: Xiaorong Xu

Received June 13, 2019; revised August 17, 2019; accepted August 29, 2019; published January 31, 2020

Abstract

In an underlay cognitive simultaneous wireless information and power transfer (SWIPT) network, communication from secondary user (SU) to secondary destination (SD) is accomplished with decode-and-forward (DF) relays. Multiple energy-constrained relays are assumed to harvest energy from SU via power splitting (PS) protocol and complete SU secure information transmission with beamforming. Hence, physical layer security (PLS) is investigated in cognitive SWIPT network. In order to interfere with eavesdropper and improve relay's energy efficiency, a destination-assisted jamming scheme is proposed. Namely, SD transmits artificial noise (AN) to interfere with eavesdropping, while jamming signal can also provide harvested energy to relays. Beamforming vector and power splitting ratio are jointly optimized with the objective of SU secrecy capacity maximization. We solve this non-convex optimization problem via a general two-stage procedure. Firstly, we obtain the optimal beamforming vector through semi-definite relaxation (SDR) method with a fixed power splitting ratio. Secondly, the best power splitting ratio can be obtained by one-dimensional search. We provide simulation results to verify the proposed solution. Simulation results show that the scheme achieves the maximum SD secrecy rate with appropriate selection of power splitting ratio, and the proposed scheme guarantees security in cognitive SWIPT networks.

Keywords: Physical Layer Security (PLS), Simultaneous Wireless Information and Power Transfer (SWIPT), Artificial Noise (AN), Power Splitting (PS), Beamforming

---

This research work was supported by the Program of Zhejiang Provincial Natural Science Foundation of China (Grant No. LY19F010011), the Cooperation Program of China Scholarship Council (CSC) and Department of Education of Zhejiang Province (CSC No. 201908330543), and 2017 Excellent Backbone Teacher Support Program in Hangzhou Dianzi University.

http://doi.org/10.3837/tiis.2020.01.001 **ISSN : 1976-7277**

1. Introduction

A large quantity of bandwidth is idle and only a little bandwidth is frequently utilized in accordance with traditional spectrum allocation policy. Cognitive Radio (CR) is proposed as a potential technology to solve spectrum scarcity problem [1]. There are two classic models of cognitive radio. One is underlay spectrum sharing model and the other is overlay spectrum sharing model. In underlay spectrum sharing model, even if primary user (PU) is working, secondary user (SU) can transmit signal simultaneously under the licensed PU spectrum [2]. For underlay CR design, the interference from SUs' communication must be tolerable to PU. Another overlay spectrum sharing model is to allow SUs to access spectral bands opportunistically while PU is idle [3]. Obviously, underlay spectrum sharing model is constrained by interference regulations, while overlay spectrum sharing model depends on accurate spectrum detections. Hence, CR has been widely investigated in wireless sensor networks and cooperative relay networks for spectral efficiency improvement [4-5].

Meanwhile, the escalating number of wireless services and the huge demand for high data rate have also led to a sharp increase in power consumption, resulting in energy shortages, especially for the energy-constrained devices such as battery-powered mobile phones [5-9]. The novel technology of simultaneous wireless information and power transfer (SWIPT) has recently attracted research attention from academia and has been seen as a promising technology that is expected to solve energy shortage problem [10]. In general, there are two kinds of protocols in SWIPT technology, namely, power splitting (PS) and time switching (TS) [11]. With TS protocol, source transmits energy through radio frequency (RF) signal to receiver in first phase and the information will be transmitted in the remaining phase. With PS protocol, the receiver will set a factor to split the received signal into two streams, one for storing energy and the other for demodulating signals.

In order to jointly improve energy efficiency and spectral efficiency, many researchers have recently focused on how to combine EH and CR [12-14]. In [15], underlay CR-EH communication system consisting of cognitive transmitter (CT), cognitive relay and cognitive destination (CD) is studied. The authors derive a closed-form expression of system outage probability. In [16], authors further illustrate outage performance analysis by jointly considering PU' s interference threshold, CT's transmission power constraint and path loss factors. In [17], authors analyze outage probability of EH-CR cooperative network, where CT collects energy from primary transmitter (PT) and acts as relay during PT's signal transmission. However, because of the broadcast characteristics of radio networks and CRN's inherent characteristics, illegal users can access PU's channel or change the wireless environment illegitimately. As a result, legitimate SU cannot access the licensed bands or be intercepted [18]. Thus, it is extremely important of communication security in SWIPT-CR network.

The demand of secure wireless communication has been focused on by ever-increasing public attentions. For example, privacy-aware users are evaluated by quality-of-experience (QoE) guarantee [19]. Physical layer security (PLS) based on wireless physical layer characteristics is promising to prevent eavesdropping in wireless network [20]. In [21], Wyner put forward a classical wiretap model, which consists of source, destination and eavesdropper. Information sent from the source to the destination may be intercepted by an eavesdropper. In addition, Wyner introduces the concept of secret capacity, which is described as the maximum achievable data rate for secret transmission from source to destination. For a basic wire-tap channel, the secrecy capacity is defined as the difference in channel capacity between the legitimate channel from source to destination and the illegal channel from source to eavesdropper [22].

A. Related Works

Presently, PLS of wireless communication networks combining with EH and CR has been paid much attention by researchers. Ref. [18] studies a secure SWIPT-CR communication system and proposes a secure resource allocation algorithm for secondary networks. In [23], the authors study the design of artificial noise (AN) and the secure pre-coding algorithm with a guaranteed convergence performance in a multiple-input multiple-output (MIMO) SWIPT-CR communication system. The authors construct the optimal problem as secrecy rate maximization (SRM). They propose an iterative algorithm to solve the problem. Ref. [24] studies the physical layer security in a SWIPT-CR system and obtains a closed-form expression for the secrecy outage probability. Ref. [25] focuses on the designing of robust secure beamforming scheme in multiple-input single-output (MISO) SWIPT-CR system for secure SU transmission. It assumes that SU can harvest energy from cognitive base station (CBS) and use PU licensed spectrum in underlay spectrum sharing model. The authors find that there exists a trade-off between the security of the secondary network and the energy harvested by EH receivers with a max-min fairness criterion. In [26], the authors study the PLS performance of an EH underlay CR system model which is similar to [25]. But the SU in [26] collects energy from the PU rather than energy from the CBS in [25]. Ref. [27] considers a destination-assisted SWIPT-CR system. In this system, SU harvests energy from PU and acts as a relay to forward the information message of the PU.

B. Motivation and Contribution

Since eavesdroppers may intercept information in the secondary network, it is necessary to study the secure communication of SUs. Motivated by the discussion shown above, different from [23-24], we pay attention to enhancing secrecy capacity in cognitive SWIPT network. The main contributions of our work can be summarized as follows. PLS for SWIPT underlay cognitive system consisting of a SU, a SD and multiple SWIPT cognitive relays which are powered by the energy harvested from RF signal are investigated. Similar to [27], in order to interfere with eavesdropper and improve the energy harvested by the relay, a destination-assisted jamming scheme is proposed. In this scheme, when SU broadcasts its signal, secondary destination (SD) will transmit AN to interfere with the eavesdropper. In addition, the interfering signal can also provide energy to SWIPT relays. Different from [27], we analyze secrecy performance in an underlay SWIPT-CR system, where the spectrum sharing model in [27] is neither underlay nor overlay. Moreover, we consider the problem of interference from SU to PU's communication. In order to reduce the harmful interference caused by SU, the constraint SU transmission power is taken into account. With the transmission power constraints on SU, we jointly design the beamforming vector and power splitting ratio to maximize the secrecy rate in SD. Due to the non-convexity of the optimization problem, we propose a general two-stage process. Namely, for a given power splitting ratio, the optimal beamforming vector is studied. Then, the best power splitting ratio can be obtained by one-dimensional search. Finally, in order to achieve secure communication, we also examine the conventional relay selection (CRS) scheme to improve PLS performance.

The rest structure of this paper is set as follows. In Section II, we introduce system model of this paper and the proposed optimization problem. In Section III, the solution of optimization problem is presented. Then, we analyze the PLS performance in accordance with simulation results given in the Section IV. Finally, we summarize the whole paper in Section V. A summary of the fundamental symbols used in paper is provided in **Table 1.**

Table 1. List of symbols.

Symbols	Descriptions
R_i	The i-th relay (i = 1, 2, …, M)
R_j	The j-th relay (the selected relay)
$\boldsymbol{g}_i$, $\boldsymbol{h}_i$, $\boldsymbol{q}_j$, $\boldsymbol{z}_j$	The channel coefficient vector
α , β	The channel coefficient
$\boldsymbol{n}_{\mathrm{c}}$, $\boldsymbol{n}_i$	The noise vectors
n_{E1} , n_{E2} , n_{D}	The noise variable
$\boldsymbol{w}_{\mathrm{D}}$, $\boldsymbol{w}_i$	The beamforming vector
ρ	The power splitting ratio
η	The energy transduction efficiency
Γ	The tolerable interference power at PD
$\mathrm{E}[x]$	Expectation of x
$\boldsymbol{w}^{\mathrm{H}}$	Hermitian transpose of $\boldsymbol{w}$
$\lVert\boldsymbol{w}\rVert$	Euclidean norm of $\boldsymbol{w}$
$\lvert x \rvert$	Absolute value of x
$\{x\}_+$	Maximum value of 0 and x
$\mathrm{Tr}(\boldsymbol{W})$	The trace of $\boldsymbol{W}$
$\boldsymbol{I}_N$	N- dimensional identity matrix
$n \sim CN(\mu, \sigma^2)$	A circularly symmetric complex Gaussian distributed variable with mean μ and covariance σ^2

2. System Model

Consider a cognitive SWIPT decode-and-forward (DF) relay network with underlay spectrum sharing model, as shown in **Fig. 1**. In the primary network, primary destination (PD) receives signals transmitted from the PU. At the same time, SU transmitter sends its secret information to SD. We assume that SU cannot directly transfer information to SD due to wireless channel attenuation. The eavesdropper EVE will overhear the transmitted information. The communication between SU and SD is divided into two phases. SU is allowed to simultaneously transmit in the licensed PU spectrum, provided that SU to PU interference level is below a predefined threshold.

Notice that M relays denoted by energy-limited R_i (i = 1, 2, …, M) that equipped with N antennas are used to assist SU's data transmission with DF protocol. We assume that R_i is only powered by the information stream from the SU and the interference stream from the SD. Furthermore, the interference flow can be used to interfere with the tapping of eavesdropper EVE. Channel state information (CSI) of all transmit links are assumed to be Rayleigh fading channels. Furthermore, we assume that all CSI, including the wiretap channel, is available [28]. When the eavesdropper is active and its transmissions can be monitored, we can obtain the eavesdropper's CSI [29]. For example, eavesdropper is a user in network but do not get the authorization of the current services, e.g., Pay-TV broadcast services [30].

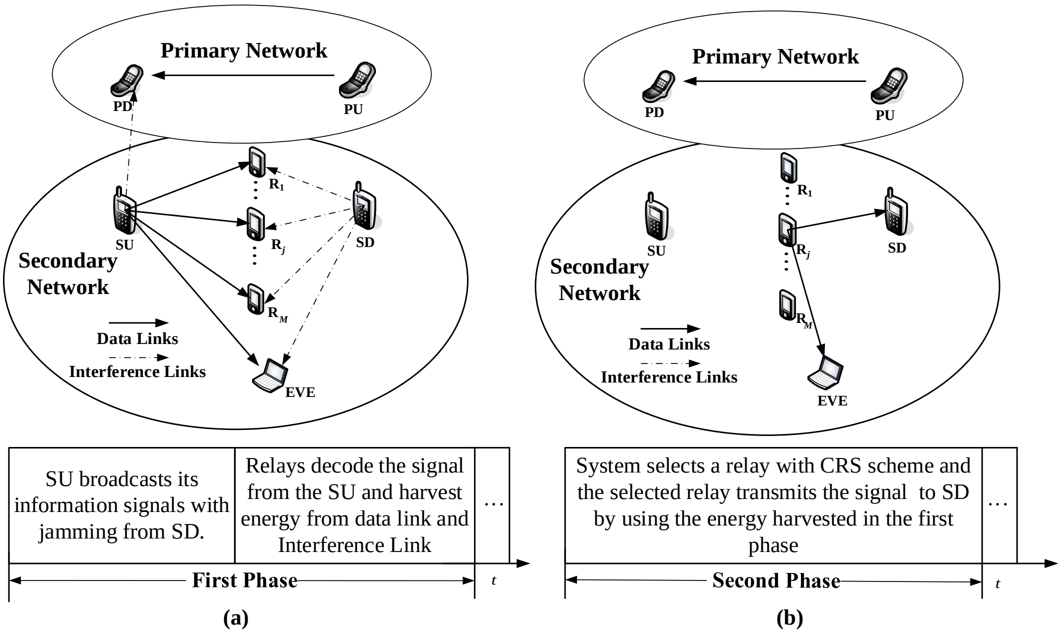

Fig. 1. SWIPT undelay CR system model and the framework of transmission.

System model and frame structure of transmission are shown in **Fig. 1**. It should be noted that the frame work is divided into two phases. Similar to [24], we assume that SD, EVE, and all the SWIPT relays are far from PU so that we can ignore the interference from PU to these nodes. Similarly, we do not consider the interference from relays and SD to PD. Since the distance is too far, relays can't get energy from the signal sent by PU. However, it is noticeable that we can not ignore the interference from SU to PD. Because it is generally assumed that SU uses a large transmit power to meet the needs of information and energy transmission. Hence, it will cause interference to PD due to the high transmit power of the SU.

Fig. 1 (a) shows the first phase of transmission framework. In the first phase, SU broadcasts its information signals to relays with power P_{S} ($P_{\mathrm{S}} \le \Gamma / X$, where Γ is the tolerable interference power at PD and X is the gain of the channel from SU to PD) under the jamming of AN transmitted by SD with power P_{D}. Suppose that the transmit signal x_{S} and AN x_{D} have the unit energy denoted as $\mathrm{E}[|x_{\mathrm{S}}|^2] = \mathrm{E}[|x_{\mathrm{D}}|^2] = 1$, signal received at R$_i$ can be expressed as

$$\boldsymbol{y}_{\mathrm{i}} = \sqrt{P_{\mathrm{S}}}\boldsymbol{h}_i x_{\mathrm{S}} + \sqrt{P_{\mathrm{D}}}\boldsymbol{g}_i x_{\mathrm{D}} + \boldsymbol{n}_i \tag{1}$$

where $\boldsymbol{h}_i$ and $\boldsymbol{g}_i$ represent the channel coefficients of SU to R$_i$, SD to R$_i$, respectively; $\boldsymbol{n}_i$ denotes $N \times 1$ circularly symmetric complex Gaussian (CSCG) noise vector with zero mean and covariance $\sigma_i^2 \boldsymbol{I}_N$ at R$_i$, i.e. $\boldsymbol{n}_i \sim CN(0, \sigma_i^2 \boldsymbol{I}_N)$.

Since relays in secondary network are SWIPT node with PS receiving equipment, the received signal is split into two streams, ρ portion of the received power is used for information-decoding (ID) part to decode information and the rest portion will be used as EH part for energy storage.

The received signal for EH at R$_i$ can be written as

$$\boldsymbol{y}_i^{\mathrm{EH}} = \sqrt{1-\rho}(\sqrt{P_{\mathrm{S}}}\boldsymbol{h}_i x_{\mathrm{S}} + \sqrt{P_{\mathrm{D}}}\boldsymbol{g}_i x_{\mathrm{D}} + \boldsymbol{n}_i) \tag{2}$$

(3)

Energy harvested by R_i is expressed as

$$P_i = (1-\rho)\eta(P_{\mathrm{S}}\|\boldsymbol{h}_i\|^2 + P_{\mathrm{D}}\|\boldsymbol{g}_i\|^2 + \sigma_i^2) \tag{4}$$

where η $(0 \le \eta \le 1)$ is denoted as energy transduction efficiency.

The received signal for ID at R_i can be given as

$$\boldsymbol{y}_i^{\mathrm{ID}} = \sqrt{\rho}(\sqrt{P_{\mathrm{S}}}\boldsymbol{h}_i x_{\mathrm{S}} + \sqrt{P_{\mathrm{D}}}\boldsymbol{g}_i x_{\mathrm{D}} + \boldsymbol{n}_i) + \boldsymbol{n}_{\mathrm{c}} \tag{5}$$

where $\boldsymbol{n}_{\mathrm{c}}$ denotes the $N \times 1$ circuit noise vector generated by the signal frequency conversion from RF to baseband. For simplicity, we assume that circuit noise vectors at all relays are subject to $\boldsymbol{n}_{\mathrm{c}} \sim CN(0, \sigma_{\mathrm{c}}^2 \boldsymbol{I}_N)$.

To avoid the influence of x_{D} on R_i, zero forcing (ZF)-based beamforming scheme is implemented. Applying the receiver vector $\boldsymbol{w}_i\,(\|\boldsymbol{w}_i\|^2 = 1; i = 1, 2, \cdots, M)$ which lies in the null space of $\boldsymbol{g}_i$, i.e. $\boldsymbol{w}_i^{\mathrm{H}}\boldsymbol{g}_i = 0$. The estimated signal at R_i can be expressed as

$$y_i = \boldsymbol{w}_i^{\mathrm{H}}[\sqrt{\rho}(\sqrt{P_{\mathrm{S}}}\boldsymbol{h}_i x_{\mathrm{S}} + \sqrt{P_{\mathrm{D}}}\boldsymbol{g}_i x_{\mathrm{D}} + \boldsymbol{n}_i) + \boldsymbol{n}_{\mathrm{c}}] \tag{6}$$

Thus, we can get the Signal to Interference plus Noise Ratio (SINR) in R_i

$$\gamma_i = \frac{\rho P_{\mathrm{S}}|\boldsymbol{w}_i^{\mathrm{H}}\boldsymbol{h}_i|^2}{\rho(P_{\mathrm{D}}|\boldsymbol{w}_i^{\mathrm{H}}\boldsymbol{g}_i|^2 + \rho\sigma_i^2) + \sigma_{\mathrm{c}}^2} \tag{7}$$

In order to maximize the SINR of R_i, the optimization problem is written as

$$\begin{aligned} &\max_{\boldsymbol{w}_i}\ \gamma_i \\ &\text{s.t.}\quad \boldsymbol{w}_i^{\mathrm{H}}\boldsymbol{g}_i = 0 \\ &\qquad\ \ \boldsymbol{w}_i^{\mathrm{H}}\boldsymbol{w}_i = 1 \end{aligned} \tag{8}$$

The problem in (7) is also called the null-steering beamformer and we can get the optimal solution from [29] as

$$\boldsymbol{w}_i = \frac{(\boldsymbol{I}_N - \boldsymbol{S}_i)\boldsymbol{h}_i}{\|(\boldsymbol{I}_N - \boldsymbol{S}_i)\boldsymbol{h}_i\|} \tag{9}$$

where $\boldsymbol{S}_i = \boldsymbol{g}_i(\boldsymbol{g}_i^{\mathrm{H}}\boldsymbol{g}_i)^{-1}\boldsymbol{g}_i^{\mathrm{H}}$.

Then, we consider the signal received at EVE from SU, which can be obtained as

$$y_{\mathrm{E1}} = \sqrt{P_{\mathrm{S}}}\alpha x_{\mathrm{S}} + \sqrt{P_{\mathrm{D}}}\beta x_{\mathrm{D}} + n_{\mathrm{E1}} \tag{10}$$

where α and β denote SU to EVE channel coefficient and SD to EVE channel coefficient respectively; $n_{\mathrm{E1}} \sim CN(0, \sigma_{\mathrm{E1}}^2)$ is a CSCG random noise variable with zero mean and variance σ_{E1}^2 received by EVE.

Hence, SINR at EVE can be written as

$$\gamma_{\mathrm{E1}} = \frac{P_{\mathrm{S}}|\alpha|^2}{P_{\mathrm{D}}|\beta|^2 + \sigma_{\mathrm{E1}}^2} \tag{11}$$

SU chooses the j-th relay R_j by using the CRS scheme [31]. Mathematically, the relay selection criterion is given by

$$\mathrm{R}_j = \arg\max_{\mathrm{R}_i,\, i=1,2,\cdots,M} \gamma_i \tag{12}$$

Substitute (8) into (6), (11) can be rewritten as

$$\mathrm{R}_j = \arg\max_{\mathrm{R}_i,\, i=1,2,\cdots,M} \|\boldsymbol{h}_i\|^2 \tag{13}$$

Fig. 1 (b) shows the second phase of transmission framework. In the second phase, R_j transmit x_S to SD with energy collected in the first phase. The transmit data at R_j is given by

$$\boldsymbol{x}_j = \sqrt{P_j}\boldsymbol{w}_\mathrm{D} x_\mathrm{S} \tag{14}$$

where $\boldsymbol{w}_\mathrm{D} \in \mathbb{C}^{N\times 1}$ denotes the beamforming vector for SD.

Then, we can get the expression of received signal

$$y_\mathrm{D} = \sqrt{P_j}\boldsymbol{q}_j^\mathrm{H}\boldsymbol{w}_\mathrm{D} x_\mathrm{S} + n_\mathrm{D} \tag{15}$$

where $\boldsymbol{q}_j$ is the channel gain coefficients from R_j to SD; $n_\mathrm{D} \sim CN(0,\sigma_\mathrm{D}^2)$ denotes a CSCG random variable received by SD.

According to (14), SINR at SD can be shown as

$$\gamma_\mathrm{D} = (1-\rho)P_\mathrm{r} \,|\boldsymbol{q}_j^\mathrm{H}\boldsymbol{w}_\mathrm{D}|^2 / \sigma_\mathrm{D}^2 \tag{16}$$

where $P_\mathrm{r} = \eta(P_\mathrm{S}\|\boldsymbol{h}_j\|^2 + P_\mathrm{D}\|\boldsymbol{g}_j\|^2 + \sigma_j^2)$.

In the same way, we can easily obtain the expression of received signal at EVE

$$y_\mathrm{E2} = \sqrt{P_j}\boldsymbol{z}_j^\mathrm{H}\boldsymbol{w}_\mathrm{D} x_\mathrm{S} + n_\mathrm{E2} \tag{17}$$

where $\boldsymbol{z}_j$ represents channel fading coefficient from R_j to EVE; $n_\mathrm{E2} \sim CN(0,\sigma_\mathrm{E2}^2)$ represents a CSCG random variable at EVE. SINR at EVE can be expressed as

$$\gamma_\mathrm{E2} = (1-\rho)P_\mathrm{r} \,|\boldsymbol{z}_j^\mathrm{H}\boldsymbol{w}_\mathrm{D}|^2 / \sigma_\mathrm{E2}^2 \tag{18}$$

Similar to [32], we assume that R_j and SD can successfully decode the message. For a two-hop DF-based relay channel, the achievable secrecy rate at SD can be written as

$$R_\mathrm{S} = \frac{1}{2}\{\min[\log_2(1+\gamma_j), \log_2(1+\gamma_\mathrm{D})] - \log_2(1+\gamma_\mathrm{E1}+\gamma_\mathrm{E2})\}_+ \tag{19}$$

The security rate refers to the transmission rate with the condition that eavesdropper cannot eavesdrop the legitimate information [32]. Then, we mainly study the joint design of power splitting ratio ρ and beamforming vector $\boldsymbol{w}_\mathrm{D}$ to maximize the achievable secrecy rate at SD. Hence, we formulate the optimum problem as below.

$$\mathcal{P}1: \max_{\boldsymbol{w}_\mathrm{D}, 0\le\rho\le 1} R_\mathrm{S} \tag{19a}$$

$$\text{s.t.} \quad \|\boldsymbol{w}_\mathrm{D}\|^2 \le 1 \tag{19b}$$

where $\|\boldsymbol{w}_\mathrm{D}\|^2 \le 1$ denotes R_j transmission power constraint.

3. Optimization Solution

It is apparent that optimum Problem (P1) shown in (19) is non-convex, because both the objective function and the constraint condition are non-convex with respect to ρ and $\boldsymbol{w}_\mathrm{D}$. In this section, we propose a general algorithm based on SDR to solve Problem (P1) with two-stage procedure. We find that the constraint condition shown in (19) is only related with beamforming vector $\boldsymbol{w}_\mathrm{D}$. Hence, we can firstly get the optimal $\boldsymbol{w}_\mathrm{D}$ for a given power splitting ratio ρ. Next, the optimal ρ can be searched through the bisection method.

When relay applies DF protocol, the total channel capacity of the secondary network depends on the link with the smaller capacity in SU to R_j and R_j to SD. Thus, the system capacity achieves the max value with $\gamma_j = \gamma_\mathrm{D}$ [32]. Moreover, we note that γ_j is only depend on variable ρ from (6). Then, with fixed ρ, we have Problem (P2)

$$\mathcal{P}2: \max_{\boldsymbol{w}_{\mathrm{D}}} \log_2(1+\gamma_{\mathrm{D}})-\log_2(1+\gamma_{\mathrm{E1}}+\gamma_{\mathrm{E2}}) \tag{20a}$$

$$\text{s.t.} \quad \|\boldsymbol{w}_{\mathrm{D}}\|^2 \le 1 \tag{20b}$$

If the optimum Problem (P2) is resolved, we can obtain the optimal $\boldsymbol{w}_{\mathrm{D}}$ for a given power splitting ratio ρ. Since if $\gamma_j=\gamma_{\mathrm{D}}$, Problem (P1) and (P2) are equivalent, so that the optimal ρ can be searched with the equation relationship $\gamma_j=\gamma_{\mathrm{D}}$. Next, we propose an SDR-based algorithm to solve Problem (P2). From (10), it is obvious that γ_{E1} is a constant. Hence, we focus on γ_{E2} and give the following proposition shown as below.

Proposition 1: For a given Problem (P2), there always exists SINR value threshold $\gamma_{\mathrm{e}}(\gamma_{\mathrm{e}}>0)$, such that the Problem (P3) as follow can get a solution that same as (P2).

$$\mathcal{P}3: \max_{\boldsymbol{w}_{\mathrm{D}}} \log_2(1+\gamma_D) \tag{21a}$$

$$\text{s.t.} \quad \gamma_{\mathrm{E2}} \le \gamma_{\mathrm{e}} \tag{21b}$$

$$\|\boldsymbol{w}_{\mathrm{D}}\|^2 \le 1 \tag{21c}$$

Proof: Refer to Appendix A.

The Problem (P3) also can be reformulated as

$$\mathcal{P}4: \max_{\boldsymbol{w}_{\mathrm{D}}} (1-\rho)P_{\mathrm{r}}|\boldsymbol{q}_j^{\mathrm{H}}\boldsymbol{w}_{\mathrm{D}}|^2/\sigma_{\mathrm{D}}^2 \tag{22a}$$

$$\text{s.t.} \quad (1-\rho)P_{\mathrm{r}}|\boldsymbol{z}_j^{\mathrm{H}}\boldsymbol{w}_{\mathrm{D}}|^2/\sigma_{\mathrm{E2}}^2 \le \gamma_{\mathrm{e}} \tag{22b}$$

$$\|\boldsymbol{w}_{\mathrm{D}}\|^2 \le 1 \tag{22c}$$

We can observe that Problem (P4)'s objective function does not involve a logarithmic function while that in Problem (P3) does, which means there exists difference between these two problems. It is denoted that Problem (P3) and Problem (P4) are equivalent, since they have the same optimal solution of $\boldsymbol{w}_{\mathrm{D}}$.

With a given SINR value threshold $\gamma_{\mathrm{e}}(\gamma_{\mathrm{e}}>0)$, we define $g(\gamma_{\mathrm{e}})$ as the optimal solution of Problem (P4). Then, we have following proposition.

Proposition 2: Problem (P4-EQV) can get a solution that same as Problem (P2).

$$\mathcal{P}4\text{-EQV}: \max_{\gamma_{\mathrm{e}}>0} R(\gamma_{\mathrm{e}}) := \log_2(1+g(\gamma_{\mathrm{e}}))-\log_2(1+\gamma_{\mathrm{E1}}+\gamma_{\mathrm{e}}) \tag{23}$$

Proof: Refer to Appendix B.

Proposition 2 establishes the relationship between Problem (P2) and the auxiliary function $g(\gamma_{\mathrm{e}})$ related to Problem (P4). The equivalence between Problem (P4-EQV) and (P2) means that by solving the optimal γ_{e} in Problem (P4-EQV), we can obtain an optimal beamforming vector $\boldsymbol{w}_{\mathrm{D}}$ where $g(\gamma_{\mathrm{e}})$ is an embedded optimization problem of $\boldsymbol{w}_{\mathrm{D}}$ in Problem (P4-EQV). Comparing Problem (P2) and its equivalent Problem (P4-EQV), we can find that the search of optimal beamforming vector $\boldsymbol{w}_{\mathrm{D}}$ is equivalent to search the corresponding value γ_{e}.

We assume that γ_{e}^* is the optimal solution for the Problem (P4-EQV). As denoted above, with $\gamma_{\mathrm{e}}=\gamma_{\mathrm{e}}^*$, Problem (P2) can get a solution that same as Problem (P4). Hence, we have following two-step method to solve the Problem (P2): Firstly, by solving (P4) with any γ_{e}, $g(\gamma_{\mathrm{e}})$ can be obtained. Secondly, we can get the best γ_{e} in Problem (P4-EQV) by one-dimension search in the range $\gamma_{\mathrm{e}}>0$. Therefore, we focus on how to solve Problem (P4) in the rest of this section.

Note that Problem (P4) is still non-convex. The SDR of Problem (P4) can be written as the equivalent problem by ignoring the rank-one constraint on $\boldsymbol{W}_{\mathrm{D}}$ shown as below, where $\boldsymbol{Q}_j = \boldsymbol{q}_j\boldsymbol{q}_j^{\mathrm{H}}$, $\boldsymbol{Z}_j = \boldsymbol{z}_j\boldsymbol{z}_j^{\mathrm{H}}$, $\boldsymbol{W}_{\mathrm{D}} = \boldsymbol{w}_{\mathrm{D}}\boldsymbol{w}_{\mathrm{D}}^{\mathrm{H}}$. This is a convex semi-definite programming (SDP) that can be efficiently solved by a convex optimization solver (such as the CVX tool).

$$\mathcal{P}4\text{-SDR}: \quad \max_{\boldsymbol{W}_{\mathrm{D}}} \ (1-\rho)P_{\mathrm{r}}\mathrm{Tr}(\boldsymbol{Q}_j\boldsymbol{W}_{\mathrm{D}})/\sigma_{\mathrm{D}}^2 \tag{24a}$$

$$\text{s.t.} \quad (1-\rho)P_{\mathrm{r}}\mathrm{Tr}(\boldsymbol{Z}_j\boldsymbol{W}_{\mathrm{D}}) \le \gamma_{\mathrm{e}}\sigma_{\mathrm{E2}}^2 \tag{24b}$$

$$\mathrm{Tr}(\boldsymbol{W}_{\mathrm{D}}) \le 1 \tag{24c}$$

Proposition 3: the optimal solution of Problem (P4-SDR) $\boldsymbol{W}_{\mathrm{D}}^*$ always satisfies $\mathrm{rank}(\boldsymbol{W}_{\mathrm{D}}^*) = 1$.

Proof: Refer to Appendix C.

According to *Proposition 3*, if the optimal solution $\boldsymbol{W}_{\mathrm{D}}^*$ of Problem (P4-SDR) can be obtained, we can get $\boldsymbol{w}_{\mathrm{D}}^*$ through the eigenvalue decomposition (EVD) of $\boldsymbol{W}_{\mathrm{D}}^*$ with $\mathrm{rank}(\boldsymbol{W}_{\mathrm{D}}^*) = 1$. As a result, (P4) can be solved with a fixed γ_{e}. Then, we will derive the optimal γ_{e}^* shown as below.

We define λ_1 and λ_2 to be the dual variables of (P4-SDR) that related SINR constraint of EVE and the power constraint in (24), respectively. Thus, the Lagrangian function of Problem (P4-SDR) can be constructed as

$$L(\boldsymbol{W}_{\mathrm{D}}, \lambda_1, \lambda_2, \gamma_{\mathrm{e}}) = \mathrm{Tr}(\boldsymbol{A}\boldsymbol{W}_{\mathrm{D}}) + B \tag{25}$$

where

$$\boldsymbol{A} = (1-\rho)P_{\mathrm{r}}\boldsymbol{Q}_j - \lambda_1(1-\rho)P_{\mathrm{r}}\boldsymbol{Z}_j - \lambda_2\boldsymbol{I}_N \tag{26}$$

$$B = \lambda_1\gamma_{\mathrm{e}}\sigma_{\mathrm{E2}}^2 + \lambda_2 \tag{27}$$

The Largrangian dual function is given by

$$F(\lambda_1, \lambda_2, \gamma_{\mathrm{e}}) = \max_{\boldsymbol{W}_{\mathrm{D}} \ge 0} L(\boldsymbol{W}_{\mathrm{D}}, \lambda_1, \lambda_2, \gamma_{\mathrm{e}}) \tag{28}$$

Since the Problem (P4-SDR) is convex and its duality gap is zero and the strong duality holds [33]. Therefore,

$$g(\gamma_{\mathrm{e}}) = \min_{\lambda_1 \ge 0, \lambda_2 \ge 0} F(\lambda_1, \lambda_2, \gamma_{\mathrm{e}}) \tag{29}$$

According to [34], $R(\gamma_{\mathrm{e}})$ in (23) has only one maximum point over $\gamma_{\mathrm{e}} > 0$. Thus, we can find the optimal γ_{e}^* by one-dimensional search. Therefore, we can find the optimal value along the gradient direction of γ_{e}.

By (23), we can express the gradient of the gradient of γ_{e} as

$$\frac{dR(\gamma_{\mathrm{e}})}{d\gamma_{\mathrm{e}}} = \frac{(1+\gamma_{\mathrm{E1}}+\gamma_{\mathrm{e}})dg(\gamma_{\mathrm{e}})/d\gamma_{\mathrm{e}} - (1+g(\gamma_{\mathrm{e}}))}{(1+g(\gamma_{\mathrm{e}}))(1+\gamma_{\mathrm{E1}}+\gamma_{\mathrm{e}})\ln 2} \tag{30}$$

Define λ_1^* and λ_2^* to be the optimal dual solutions of (P4-SDR). Based on (29), we can get

$$dg(\gamma_{\mathrm{e}})/d\gamma_{\mathrm{e}} = \lambda_1^*\sigma_{\mathrm{E2}}^2 \tag{31}$$

So far, Problem (P1)'s optimal solution can be derived of by fixing ρ. Then, optimal ρ can be obtained via the relationship $\gamma_j = \gamma_{\mathrm{D}}$. It can be easily observed that as ρ increases, γ_j increases and γ_{D} decreases. In addition, $\gamma_j^{\max} > \gamma_{\mathrm{D}}^{\min}$ and $\gamma_{\mathrm{D}}^{\max} > \gamma_j^{\min}$.

$$h(\rho) = \gamma_{\mathrm{D}} - \gamma_j \tag{32}$$

It is easy to conclude that, $h(\rho)$ in (32) is increasing with ρ. Hence, there is only one value of optimal ρ (ρ^*) satisfying the condition $h(\rho^*) = 0$. We can get the best value of ρ (ρ^*) by one-dimensional search.

In conclusion, we use a three-step approach to solve Problem (P1). Firstly, we fixed ρ and γ_{e} to solve the Problem (P4). Secondly, we find the optimal γ_{e}^* by one-dimensional search. Thirdly, the optimal ρ^* is obtained by bisection. At last, repeat the above steps until the problem is solved. The specific steps have been summarized in the **Table 2** show as below.

Table 2. Specific steps of searching the optimum solution for Problem (P1)

Initialize $\rho^{\min}$, $\rho^{\max}$ and tolerance δ;
while $\rho^{\max} - \rho^{\min} > \delta$ **do**
$\rho \leftarrow (\rho^{\max} + \rho^{\min})/2$
Initialize $\gamma_{\mathrm{e}}^{\min}$, $\gamma_{\mathrm{e}}^{\max}$ and tolerance ε;
while $\gamma_{\mathrm{e}}^{\max} - \gamma_{\mathrm{e}}^{\min} > \varepsilon$ **do**
$\gamma_{\mathrm{e}} \leftarrow (\gamma_{\mathrm{e}}^{\max} + \gamma_{\mathrm{e}}^{\min})/2$
Solve the Problem (P4-SDR) to obtain λ_1^*, λ_2^* and $\boldsymbol{W}_{\mathrm{D}}^*$,
Calculate $dR(\gamma_{\mathrm{e}})/d\gamma_{\mathrm{e}}$ in accordance with (30) and (31);
if $dR(\gamma_{\mathrm{e}})/d\gamma_{\mathrm{e}} > 0$ **then**
$\gamma_{\mathrm{e}}^{\min} \leftarrow \gamma_{\mathrm{e}}$;
else
$\gamma_{\mathrm{e}}^{\max} \leftarrow \gamma_{\mathrm{e}}$;
end if
end while
return $\boldsymbol{w}_{\mathrm{D}}^*$ via EVD of $\boldsymbol{W}_{\mathrm{D}}^*$;
Calculate $h(\rho)$ in accordance with (32);
if $h(\rho) > 0$ **then**
$\rho^{\min} \leftarrow \rho$;
else
$\rho^{\max} \leftarrow \rho$;
end if
end while

4. Simulation Results and Performance Analysis

In this section, simulation results are given to verify PLS performance of the proposed scheme in this paper. The impacts of tolerable interference power at PD Γ, artificial noise power P_{D} and the number of relays M on the SD achievable secrecy rate are investigated with performance analysis shown as below. The specific values assigned to system parameters are originated from [27], [35-37].

Simulation parameters are set as follows. In order to simplify the process without losing generality, we set the noise power of all nodes to 0dBm and set the channel gain of SU to PD as 1. Other channel vectors and coefficients are randomly generated from i.i.d. Rayleigh fading with the respective average power values. According to [35], we set the path loss exponent to be 3. In the secondary network, the distance between SU and EVE is set to be 6m, other distances are all set to be 4m [27]. There are M = 5 relays in the secondary network and each relay is equipped with N = 4 antennas, while other nodes are equipped with single antenna. The transmission power of SD is set to be $P_{\mathrm{D}} = 20\mathrm{dBm}$ and the tolerable interference power at PD is set to be $\Gamma = 30\mathrm{dBm}$. According to [36], the energy-harvesting efficiency η is set as 0.8. In order to better observe the impact of SU transmit power on system performance, we assume that the SU transmits signal with $P_{\mathrm{S}} = \Gamma / X$.

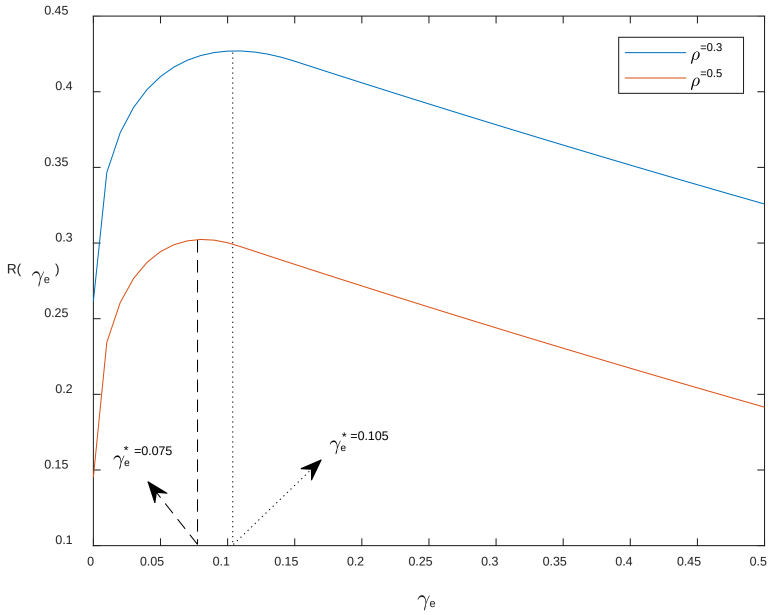

Fig. 2. $R(\gamma_{\mathrm{e}})$ versus γ_{e} (with $\rho = 0.3$ and $\rho = 0.5$)

We illustrate the two-stage optimization approach to solve Problem (P2) and Problem (P3), as proposed in Section II and Section III, respectively. **Fig. 2** shows the relationship between $R(\gamma_{\mathrm{e}})$ and $\gamma_{\mathrm{e}}(\gamma_{\mathrm{e}} > 0)$ with a fixed ρ. We can observe that with $\rho = 0.3$ and $\rho = 0.5$ (and many others used in our simulations for which the results are not shown here due to the space limitation), there is only one single optimal γ_{e} to maximize $R(\gamma_{\mathrm{e}})$, which means we can find a γ_{e} for (P3) (uniqueness of γ_{e}^* in (P3)) to solve (P2). For example, $R(\gamma_{\mathrm{e}})$ achieves the peak values with γ_{e}^*=0.105 for $\rho = 0.3$ and γ_{e}^*=0.075 for $\rho = 0.5$, respectively. **Fig. 3** and **Fig. 4** show the plot of $h(\rho)$ over $0 \le \rho \le 1$ and the relationship between R_S and ρ, respectively. It can be observed from **Fig. 3** and **Fig. 4** that the optimal point ρ^*=0.15 with $h(\rho) = 0$ can make R_S get the maximum value (uniqueness of ρ^* in (P1)).

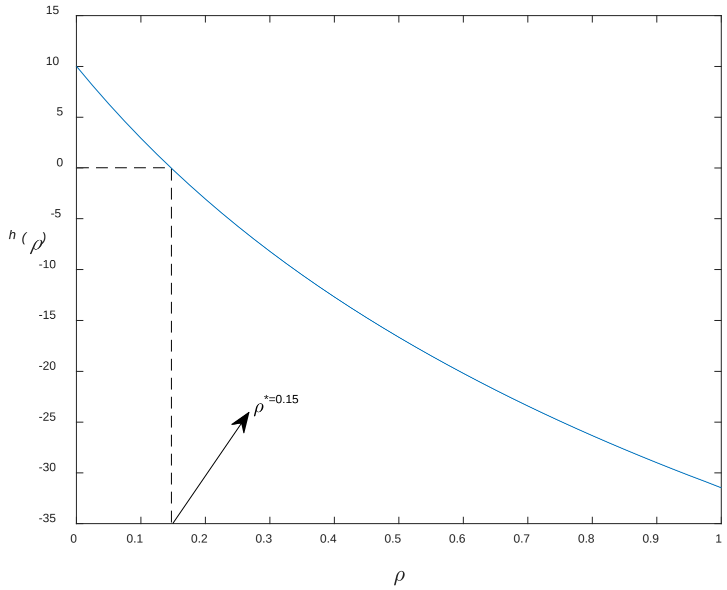

Fig. 3. $h(\rho)$ versus ρ.

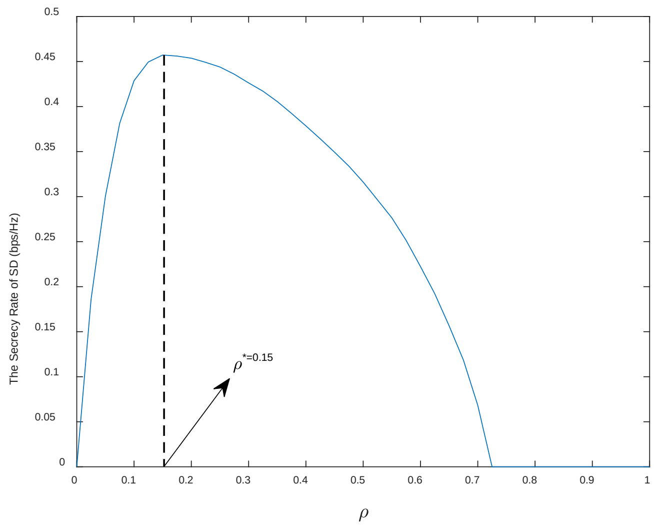

Fig. 4. R_S versus ρ.

Fig. 5 shows the secrecy rate of SD versus tolerable interference power at PD. Furthermore, for security comparison, the proposed SDR-based algorithm is compared with the ZF-based solution [37]. It can be easily observed that the achieved secrecy rates increase with the growth of tolerable interference power at PD for all schemes. From **Fig. 5**, it is obvious that the proposed SDR-based scheme outperforms ZF-based scheme when tolerable interference power is more than 10 dBm. When tolerable interference power is less than 10 dBm, SD secrecy rate performance of SDR-based scheme is slightly worse than ZF-based scheme due to the accuracy of the one-dimensional search for γ_e^*. When the tolerable interference power at PD is fixed, SD secrecy rate increases with CRS for two schemes, which verifies that the CRS in (11) is beneficial to the SD secrecy performance in the system.

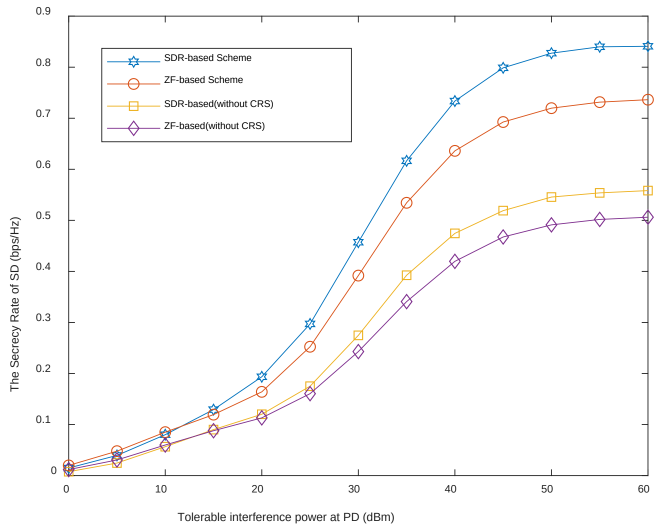

Fig. 5. Secrecy rate of SD versus tolerable interference power at PD.

Fig. 6 depicts the secrecy rate performance versus the artificial noise power at SD. From this figure, we can find that the secrecy performances with ZF-based scheme and SDR-based scheme both up with the increase of AN power at SD. It can be also observed that the performance gap between the ZF-based scheme and SDR-based scheme becomes smaller for higher P_D . The reason is that, EVE is interfered by the AN transmitted from SD in first phase. At the same time, energy harvested by optimal relay also enhances with power of AN increases, which leads to the improvement of the SINR at SD in the second phase. According to (18), when jamming power is particularly large, the secrecy rate mainly depends on SINR at relays in the first phase. Hence, the gap between the two schemes will become smaller and smaller as the power of AN increases. Moreover, in order to demonstrate the advantages of CRS, SD secrecy rate performance without CRS is also provided as comparison. It is significant that the SD secrecy performance enhances with the application of CRS.

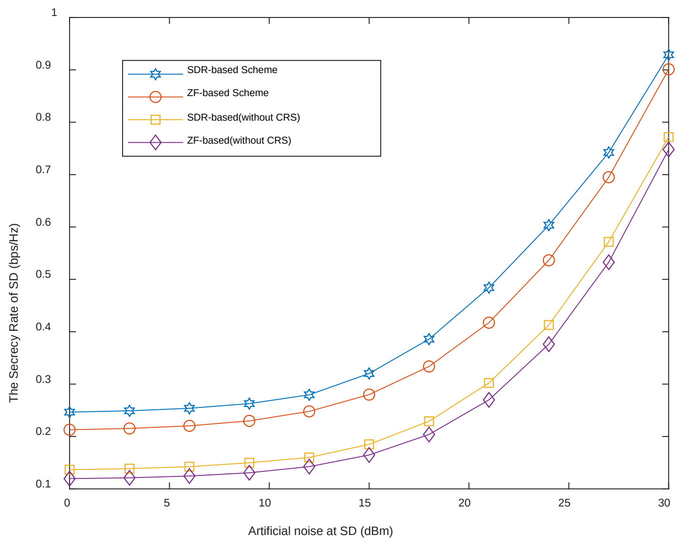

Fig. 6. Secrecy rate of SD versus the artificial noise power at SD.

Fig. 7 shows the relationship between the secrecy rate performance and the number of relays. As expected, the secrecy rate of secondary network improves with the increase of M. In addition, under the same number of relays, the performance of SDR-based scheme is further better than ZF-based scheme.

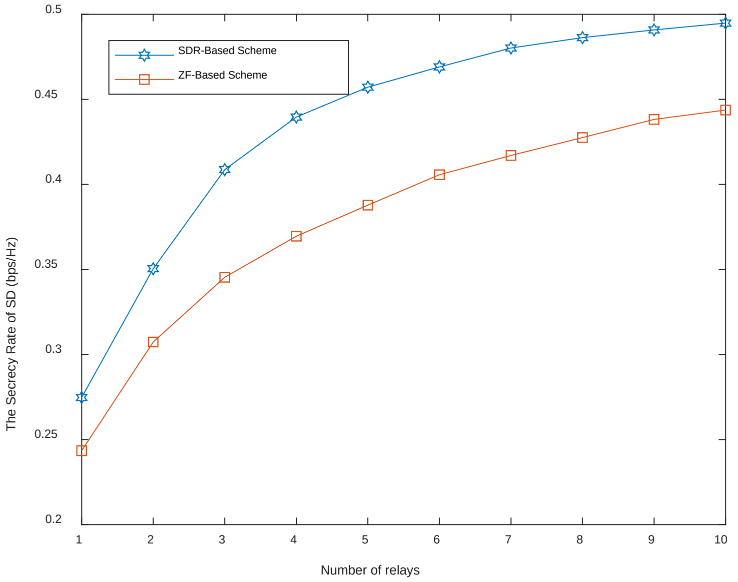

Fig. 7. Secrecy rate of SD versus number of relays.

5. Conclusions

In this paper, we have considered the physical layer security for cognitive radio cooperative systems with SWIPT technology. Under the power constraint of secondary user, the joint power split ratio and beamforming design is studied to maximize the secret information transmission rate to the secondary destination. By applying SDR method, a general two-stage procedure has been proposed to solve the formulated non-convex design problems. In addition, extensive simulation results are provided to evaluate the security performance of our proposed scheme.

Appendixes

A. Proof of Proposition 1

For the fixed ρ, we assume that $\boldsymbol{w}_{\mathrm{D}}^*$ is the optimal solution of Problem (P2) and define $\gamma_{\mathrm{e}}^* = \gamma_{\mathrm{E2}}^* = (1-\rho)P_{\mathrm{r}}|\mathbf{z}_j^{\mathrm{H}}\boldsymbol{w}_{\mathrm{D}}^*|^2/\sigma_{\mathrm{E2}}^2$. Similarly, $\boldsymbol{w}_{\mathrm{DA}}^*$ is assumed to be the Problem (P3)'s optimal solution and γ_{E2A}^* is defined as $\gamma_{\mathrm{E2A}}^* = (1-\rho)P_{\mathrm{r}}(\mathbf{z}_j^{\mathrm{H}}\boldsymbol{w}_{\mathrm{DA}}^*)^2/\sigma_{\mathrm{E2}}^2$. If $\boldsymbol{w}_{\mathrm{DA}}^*$ satisfies $\log_2(1+\gamma_{\mathrm{E1}}+\gamma_{\mathrm{E2A}}^*) > \log_2(1+\gamma_{\mathrm{E1}}+\gamma_{\mathrm{E2}}^*)$, then for the Problem (P2), solution $\boldsymbol{w}_{\mathrm{DA}}^*$ is better than $\boldsymbol{w}_{\mathrm{D}}^*$, which means that $\boldsymbol{w}_{\mathrm{D}}^*$ is not the optimal solution of Problem (P2) and does not satisfy with our assumption. Therefore, it must be $\log_2(1+\gamma_{\mathrm{E1}}+\gamma_{\mathrm{E2A}}^*) \le \log_2(1+\gamma_{\mathrm{E1}}+\gamma_{\mathrm{E2}}^*)$. Then, for $\gamma_{\mathrm{e}} = \gamma_{\mathrm{e}}^*$, $\boldsymbol{w}_{\mathrm{D}}^*$ can also be regarded as the optimal solution of Problem (P3). Hence, we have

Proposition 1.

B. Proof of Proposition 2

It is easy to see that the following problem is equivalent to Problem (P2)

$$\begin{aligned} \mathcal{P}2.1: \quad & \max_{\boldsymbol{w}_{\mathrm{D}}, 0\le\rho\le1} \frac{1+\gamma_{\mathrm{D}}}{1+\gamma_{\mathrm{E1}}+\gamma_{\mathrm{E2}}} \\ \text{s.t.} \quad & \|\boldsymbol{w}_{\mathrm{D}}\|^2 \le 1 \end{aligned} \tag{B1}$$

We assume that $\boldsymbol{w}_{\mathrm{D}}^*$ is the optimal solution of Problem (P2.1) and define $\gamma_{\mathrm{e}}^* = \gamma_{E2}^* = (1-\rho)P_{\mathrm{r}} |\boldsymbol{z}_j^{\mathrm{H}}\boldsymbol{w}_{\mathrm{D}}^*|^2 / \sigma_{\mathrm{E2}}^2$, $\gamma_D^* = (1-\rho)P_{\mathrm{r}} |\boldsymbol{q}_j^{\mathrm{H}}\boldsymbol{w}_{\mathrm{D}}^*|^2 / \sigma_{\mathrm{D}}^2$. Thus, for Problem (P2.1), the optimal objective value is $T^* = \dfrac{1+\gamma_D^*}{1+\gamma_{\mathrm{E1}}+\gamma_{\mathrm{E2}}^*}$.

Similarly, $\boldsymbol{w}_{\mathrm{D1}}^*$ is assumed to be the optimal solution of Problem (P4) at $\gamma_{\mathrm{e}} = \gamma_{\mathrm{e1}}^*$. If $\boldsymbol{w}_{\mathrm{D1}}^*$ satisfies $(1-\rho)P_{\mathrm{r}} |\boldsymbol{q}_j^{\mathrm{H}}\boldsymbol{w}_{\mathrm{D1}}^*|^2 / \sigma_{\mathrm{D}}^2 > \gamma_D^*$, for Problem (P2.1), solution $\boldsymbol{w}_{\mathrm{D1}}^*$ is better than $\boldsymbol{w}_{\mathrm{D}}^*$, which contradicts the assumption that $\boldsymbol{w}_{\mathrm{D}}^*$ is the optimal solution of Problem (P2.1). In another case, we assume that $(1-\rho)P_{\mathrm{r}} |\boldsymbol{q}_j^{\mathrm{H}}\boldsymbol{w}_{\mathrm{D1}}^*|^2 / \sigma_{\mathrm{D}}^2 < \gamma_D^*$, which contradicts the assumption that $\boldsymbol{w}_{\mathrm{D1}}^*$ is the optimal solution of Problem (P4), because $\boldsymbol{w}_{\mathrm{D}}^*$ is better. Thus, $\gamma_D^* = g(\gamma_{\mathrm{e}})$ can be obtained. For Problem (P4-EQV), T^* can be achieved with $\gamma_{\mathrm{e}} = \gamma_{\mathrm{e1}}^*$.

Furthermore, we assume that the optimal solution of Problem (P4-EQV) is γ_{e2}^* and the corresponding optimal value is T_2^*. Then, $\boldsymbol{w}_{\mathrm{D2}}^*$ is assumed to be the optimal solution of Problem (P4) with $\gamma_{\mathrm{e}} = \gamma_{\mathrm{e2}}^*$. Inequality $T_2^* \le T^*$ can be proved in follows. If $T_2^* > T^*$, then $\boldsymbol{w}_{\mathrm{D2}}^*$ is a better solution of Problem (P2.1), which contradicts the presumption that $\boldsymbol{w}_{\mathrm{D}}^*$ is the optimal solution of Problem (P2.1). Thus, it can be seen that T^* is not only achievable for Problem (P4-EQV), but also the optimal value of Problem (P4-EQV) where the optimal solution is $\boldsymbol{w}_{\mathrm{D2}}^* = \boldsymbol{w}_{\mathrm{D}}^*$ and $\gamma_{\mathrm{e2}}^* = \gamma_{\mathrm{e1}}^*$ (Note that $\boldsymbol{w}_{\mathrm{D}}$ is a hidden design variable for Problem (P4-EQV)). Hence, we have *Proposition* 2.

C. Proof of Proposition 3

The KKT conditions of Problem (P4-SDR) can be expressed as

$$\begin{aligned} \mathcal{P}2.1: \quad & \max_{\boldsymbol{w}_{\mathrm{D}}, 0\le\rho\le1} \frac{1+\gamma_{\mathrm{D}}}{1+\gamma_{\mathrm{E1}}+\gamma_{\mathrm{E2}}} \\ \text{s.t.} \quad & \|\boldsymbol{w}_{\mathrm{D}}\|^2 \le 1 \end{aligned} \tag{C1}$$

Firstly, it is easily to observe that $\mathrm{rank}(\boldsymbol{A}^*) \le N$. Then, we have *Lemma 1.*

Lemma 1: Two matrices $\boldsymbol{Y}$ and $\boldsymbol{Z}$ with the same dimension hold that $\mathrm{rank}(\boldsymbol{Y}+\boldsymbol{Z}) \ge \mathrm{rank}(\boldsymbol{Z}) - \mathrm{rank}(\boldsymbol{Y})$.

Proof: We know that if two matrices $\boldsymbol{Y}$ and $\boldsymbol{Z}$ with the same dimension, $\mathrm{rank}(\boldsymbol{Y}) + \mathrm{rank}(\boldsymbol{Z}) \ge \mathrm{rank}(\boldsymbol{Y}+\boldsymbol{Z})$ is established. Therefore, we can get $\mathrm{rank}(\boldsymbol{Y}+\boldsymbol{Z}) + \mathrm{rank}(-\boldsymbol{Y}) \ge \mathrm{rank}(\boldsymbol{Z})$. Because $\mathrm{rank}(-\boldsymbol{Y}) = \mathrm{rank}(\boldsymbol{Y})$, we have $\mathrm{rank}(\boldsymbol{Y}+\boldsymbol{Z}) \ge \mathrm{rank}(\boldsymbol{Z}) - \mathrm{rank}(\boldsymbol{Y})$.

Consider the non-trivial case where $\boldsymbol{W}_{\mathrm{D}}^{*} \neq \boldsymbol{0}$, we define $\boldsymbol{Y} = (1-\rho)P_{\mathrm{r}}\boldsymbol{Q}_{j}$, $\boldsymbol{Z} = -\lambda_{1}^{*}(1-\rho)P_{\mathrm{r}}\boldsymbol{Z}_{j} - \lambda_{2}^{*}\boldsymbol{I}_{N}$. As a result, we have

$$\mathrm{rank}(\boldsymbol{A}^{*}) = \mathrm{rank}(\boldsymbol{Y} + \boldsymbol{Z}) \geq \mathrm{rank}(\boldsymbol{Z}) - \mathrm{rank}(\boldsymbol{Y}) = N - 1 \tag{C2}$$

According to the Sylvester inequality, we have

$$\mathrm{rank}(\boldsymbol{A}^{*}) + \mathrm{rank}(\boldsymbol{W}_{\mathrm{D}}^{*}) - N \leq \mathrm{rank}(\boldsymbol{A}^{*}\boldsymbol{W}_{\mathrm{D}}^{*}) = 0 \tag{C3}$$

According to (C2) and (C3), we can get

$$N - 1 \leq \mathrm{rank}(\boldsymbol{A}^{*}) \leq N - \mathrm{rank}(\boldsymbol{W}_{\mathrm{D}}^{*}) \tag{C4}$$

Therefore, *Proposition 3* can be proved as below.

$$\mathrm{rank}(\boldsymbol{W}_{\mathrm{D}}^{*}) = 1 \tag{C5}$$

References

[1] S. Haykin, "Cognitive radio: brain-empowered wireless communications," *IEEE Journal on Selected Areas in Communications*, vol. 23, no. 2, pp. 201-220, Feb. 2005. Article (CrossRef Link)

[2] C. Tang, G. Pan and T. Li, "Secrecy outage analysis of underlay cognitive radio unit over Nakagami-*m* fading channels," *IEEE Wireless Communications Letters*, vol. 3, no. 6, pp. 609-612, Dec. 2014. Article (CrossRef Link)

[3] S. Sun, Y. Ju and Y. Yamao, "Overlay cognitive radio OFDM system for 4G cellular networks," *IEEE Wireless Communications*, vol. 20, no. 2, pp. 68-73, Apr. 2013. Article (CrossRef Link)

[4] O. B. Akan, O. B. Karli and O. Ergul, "Cognitive radio sensor networks," *IEEE Network*, vol. 23, no. 4, pp. 34-40, Jul.-Aug. 2009. Article (CrossRef Link)

[5] X. Huang, T. Han and N. Ansari, "On green-energy-powered cognitive radio networks," *IEEE Communications Surveys & Tutorials*, vol. 17, no. 2, pp. 827-842, Second Quarter 2015. Article (CrossRef Link)

[6] L. Zhou, D. Wu, J. Chen and Z. Dong, "When computation hugs intelligence: content-aware data processing for industrial IoT," *IEEE Internet of Things Journal*, vol. 5, no. 3, pp. 1657-1666, June 2018. Article (CrossRef Link)

[7] A. Bayat and S. Aïssa, "Full-duplex cognitive radio with asynchronous energy-efficient sensing," *IEEE Transactions on Wireless Communications*, vol. 17, no. 2, pp. 1066-1080, Feb. 2018. Article (CrossRef Link)

[8] L. Zhou, D. Wu, J. Chen and Z. Dong, "Greening the smart cities: energy-efficient massive content delivery via D2D communications," *IEEE Transactions on Industrial Informatics*, vol. 14, no. 4, pp. 1626-1634, April 2018. Article (CrossRef Link)

[9] C. Jiang, H. Zhang, Y. Ren and H. Chen, "Energy-efficient non-cooperative cognitive radio networks: micro, meso, and macro views," *IEEE Communications Magazine*, vol. 52, no. 7, pp. 14-20, Jul. 2014. Article (CrossRef Link)

[10] R. Zhang and C. K. Ho, "MIMO broadcasting for simultaneous wireless information and power transfer," *IEEE Transactions on Wireless Communications*, vol. 12, no. 5, pp. 1989-2001, May 2013. Article (CrossRef Link)

[11] X. Chen, Z. Zhang, H. Chen and H. Zhang, "Enhancing wireless information and power transfer by exploiting multi-antenna techniques," *IEEE Communications Magazine*, vol. 53, no. 4, pp. 133-141, Apr. 2015. Article (CrossRef Link)

[12] V. Nguyen, S. Dinh-Van and O. Shin, "Opportunistic relaying with wireless energy harvesting in a cognitive radio system," in *Proc. of 2015 IEEE Wireless Communications and Networking Conference (WCNC), New Orleans, LA*, pp. 87-92, 2015. Article (CrossRef Link)

[13] C. Xu, M. Zheng, W. Liang, H. Yu and Y. Liang, "Outage performance of underlay multihop cognitive relay networks with energy harvesting," *IEEE Communications Letters*, vol. 20, no. 6, pp. 1148-1151, Jun. 2016. Article (CrossRef Link)

[14] J. He, S. Guo, F. Wang and Y. Yang, "Relay selection and outage analysis in cooperative cognitive radio networks with energy harvesting," in *Proc. of 2016 IEEE International Conference on Communications (ICC), Kuala Lumpur*, pp. 1-6, 2016. Article (CrossRef Link)
[15] Y. Liu, S. A. Mousavifar, Y. Deng, C. Leung and M. Elkashlan, "Wireless energy harvesting in a cognitive relay network," *IEEE Transactions on Wireless Communications*, vol. 15, no. 4, pp. 2498-2508, Apr. 2016. Article (CrossRef Link)
[16] T. Le and O. Shin, "Wireless energy harvesting in cognitive radio with opportunistic relays selection," in *Proc. of 2015 IEEE 26th Annual International Symposium on Personal, Indoor, and Mobile Radio Communications (PIMRC), Hong Kong*, 2015, pp. 949-953, 2015. Article (CrossRef Link)
[17] J. He, S. Guo, G. Pan, Y. Yang and D. Liu, "Relay cooperation and outage analysis in cognitive radio networks with energy harvesting," *IEEE Systems Journal*, vol. 12, no. 3, pp. 2129-2140, Sep. 2018. Article (CrossRef Link)
[18] D. W. K. Ng, E. S. Lo and R. Schober, "Multiobjective resource allocation for secure communication in cognitive radio networks with wireless information and power transfer," *IEEE Transactions on Vehicular Technology*, vol. 65, no. 5, pp. 3166-3184, May 2016. Article (CrossRef Link)
[19] L. Zhou, D. Wu, X. Wei and Z. Dong, "Seeing isn't believing: QoE evaluation for privacy-aware users," *IEEE Journal on Selected Areas in Communications*, vol. 37, no. 7, pp. 1656-1665, July 2019. Article (CrossRef Link)
[20] D. Wang, B. Bai, W. Zhao and Z. Han, "A survey of optimization approaches for wireless physical layer security," *IEEE Communications Surveys & Tutorials*, vol.21, no.2, pp.1878-1911, Second Quarter 2019. Article (CrossRef Link)
[21] A. Wyner, "The wire-tap channel," *Bell System Technical Journal*, vol. 54, no, 8, pp. 1355-1387, 1975. Article (CrossRef Link)
[22] S. Leung-Yan-Cheong and M. Hellman, "The gaussian wire-tap channel," *IEEE Transactions on Information Theory*, vol. 24, no. 4, pp. 451-456, Jul. 1978. Article (CrossRef Link)
[23] B. Fang, Z. Qian, W. Zhong and W. Shao, "AN-aided secrecy precoding for SWIPT in cognitive MIMO broadcast channels," *IEEE Communications Letters*, vol. 19, no. 9, pp. 1632-1635, Sep. 2015. Article (CrossRef Link)
[24] A. Singh, M. R. Bhatnagar and R. K. Mallik, "Secrecy outage of a simultaneous wireless information and power transfer cognitive radio system," *IEEE Wireless Communications Letters*, vol. 5, no. 3, pp. 288-291, Jun. 2016. Article (CrossRef Link)
[25] F. Zhou, Z. Li, J. Cheng, Q. Li and J. Si, "Robust AN-aided beamforming and power splitting design for secure MISO cognitive radio with SWIPT," *IEEE Transactions on Wireless Communications*, vol. 16, no. 4, pp. 2450-2464, Apr. 2017. Article (CrossRef Link)
[26] P. Yan, Y. Zou and J. Zhu, "Energy-aware multiuser scheduling for physical-layer security in energy-harvesting underlay cognitive radio systems," *IEEE Transactions on Vehicular Technology*, vol. 67, no. 3, pp. 2084-2096, Mar. 2018. Article (CrossRef Link)
[27] R. Su, Y. Wang and R. Sun, "Destination-assisted jamming for physical-layer security in SWIPT cognitive radio systems," in *Proc. of 2018 IEEE Wireless Communications and Networking Conference (WCNC), Barcelona*, pp. 1-6, 2018. Article (CrossRef Link)
[28] Y. Liu and A. P. Petropulu, "Destination assisted cooperative jamming for wireless physical layer security," in *Proc. of 2012 IEEE International Workshop on Information Forensics and Security (WIFS), Tenerife*, pp. 282-287, 2012. Article (CrossRef Link)
[29] L. Dong, Z. Han, A. P. Petropulu and H. V. Poor, "Improving wireless physical layer security via cooperating relays," *IEEE Transactions on Signal Processing*, vol. 58, no. 3, pp. 1875-1888, Mar. 2010. Article (CrossRef Link)
[30] Y. Yang, Q. Li, W. Ma, J. Ge and M. Lin, "Optimal joint cooperative beamforming and artificial noise design for secrecy rate maximization in AF relay networks," in *Proc. of 2013 IEEE 14th Workshop on Signal Processing Advances in Wireless Communications (SPAWC), Darmstadt*, pp. 360-364, 2013. Article (CrossRef Link)

[31] S. Jia, J. Zhang, H. Zhao and R. Zhang, "Relay selection for improved security in cognitive relay networks with jamming," *IEEE Wireless Communications Letters*, vol. 6, no. 5, pp. 662-665, Oct. 2017. Article (CrossRef Link)
[32] J. Huang and A. L. Swindlehurst, "Cooperative jamming for secure communications in MIMO relay networks," *IEEE Transactions on Signal Processing*, vol. 59, no. 10, pp. 4871-4884, Oct. 2011. Article (CrossRef Link)
[33] S. Boyd and L. Vandenberghe, *Convex Optimization*, Cambridge University Press, pp. 215-288, 2004. Article (CrossRef Link)
[34] L. Liu, R. Zhang and K. Chua, "Secrecy wireless information and power transfer with MISO beamforming," *IEEE Transactions on Signal Processing*, vol. 62, no. 7, pp. 1850-1863, Apr. 2014. Article (CrossRef Link)
[35] J. Jacob, A. Panicker, J. Mathew and A. P. Vinod, "Exploration of a distributed approach for simulating spectrum sensing in cognitive radio," in *Proc. of 2011 International Conference on Communications and Signal Processing, Calicut*, pp. 250-254, 2011. Article (CrossRef Link)
[36] R. Sun, Y. Wang, X. Wang and Y. Zhang, "Transceiver design for cooperative non-orthogonal multiple access systems with wireless energy transfer," *IET Communications*, vol. 10, no. 15, pp. 1947-1955, 2016. Article (CrossRef Link)
[37] W. Lu, Y. Jiang, C. Yin, X. Tao and P. Lai, "Security beamforming algorithms in multibeam satellite systems," in *Proc. of 2017 IEEE 2nd Advanced Information Technology, Electronic and Automation Control Conference (IAEAC), Chongqing*, pp. 1272-1277, 2017. Article (CrossRef Link)

Xiaorong Xu is with the School of Communication Engineering, Hangzhou Dianzi University (HDU), Hangzhou, China, as associate professor. He received the B. Eng. degree in Communication Engineering and M. Eng. degree in Communication and Information System from HDU, Hangzhou, China, in 2004 and 2007, respectively. He received Ph.D. degree major in Signal and Information Processing from Nanjing University of Posts and Telecommunications (NUPT), Nanjing, China, in 2010. Previously, from 2011 to 2013, he was working as a postdoctoral researcher in the Institute of Information and Communication Engineering, Zhejiang University (ZJU), Hangzhou, China. During 2013-2014, he serves as a research scholar with the Electrical and Computer Engineering Department, Stevens Institute of Technology (SIT), Hoboken, NJ, USA. During 2020-2021, he serves as a China Scholarship Council (CSC)-sponsored exchange visiting scholar with Department of Electrical and Computer Engineering, McGill University, Montreal, QC, Canada. Currently, he is working as associate professor in HDU and he is an excellent backbone teacher in HDU. Dr. Xu's research interests emphasize on green wireless SWIPT networks, cognitive radio networks (CRN), cooperative communications, energy efficiency and physical layer security in SWIPT network and CRN, *etc*.

Andi Hu is with the School of Communication Engineering, Hangzhou Dianzi University (HDU), Hangzhou, China, as postgraduate student. He received the B. Eng. degree in Communication Engineering from Hangzhou Dianzi University, Hangzhou, China, in 2017. Currently, he is working toward his M. Eng. degree in Information and Communication Engineering in HDU. His research interests include green wireless SWIPT networks and physical layer security in SWIPT network, *etc*.

Yingbiao Yao is with the School of Communication Engineering, Hangzhou Dianzi University (HDU), Hangzhou, China, as professor. He received the M. Eng. degree in Communication and Information System from Xi'an Shiyou University, Xi'an, China, in 2003, He received Ph.D. degree major in Communication and Information System from Zhejiang University (ZJU), Hangzhou, China, in 2006. Since 2006, he has been with the School of Communication Engineering, HDU. During 2011-2012, he served as a research scholar with the Electrical and Computer Engineering Department, Rensselaer Polytechnic Institute, Albany, NY, USA. Currently, he is working as professor in HDU. Dr. Yao's research interests emphasize on energy efficiency and physical layer security in future wireless communications, Multiprocessor System-on-Chip (MPSoC) and solid state disk (SSD) for embedded system application, *etc*.

Wei Feng is with the School of Communication Engineering, Hangzhou Dianzi University (HDU), Hangzhou, China, as lecturer. She received the B. Eng. degree in Electronics and Information Engineering from Hubei Engineering University, Xiaogan, China, in 2005, and M. Eng. degree in Information and Communication Engineering from South China University of Technology, Guangzhou, China, in 2009. She received Ph.D. degree major in Information and Communication Engineering from South China University of Technology, Guangzhou, China, in 2014. Previously, from 2005 to 2006, she was working as an FAE in LITE-ON Technology Cooperation, Guangzhou, China. From 2009 to 2011, she was working as a network engineer in Huaxin Consulting Co. Ltd, Hangzhou, China. Currently, she is a lecturer in HDU. Dr. Feng's research interests emphasize on energy efficiency and physical layer security in future wireless communications, *etc*.